


## Article

# The Annealing Kinetics of Defects in CVD Diamond Irradiated by Xe Ions

Eugene A. Kotomin <sup>1,\*</sup>, Vladimir N. Kuzovkov <sup>1</sup>, Aleksandr Lushchik <sup>2</sup>, Anatoli I. Popov <sup>1</sup>, Evgeni Shablonin <sup>2</sup>, Theo Scherer <sup>3</sup> and Evgeni Vasil'chenko <sup>2</sup>

<sup>1</sup> Institute of Solid State Physics, University of Latvia, Kengaraga 8, LV-1063 Riga, Latvia; kuzovkov@latnet.lv (V.N.K.); popov@latnet.lv (A.I.P.)

<sup>2</sup> Institute of Physics, University of Tartu, W. Ostwald Str. 1, 50411 Tartu, Estonia; aleksandr.lushchik@ut.ee (A.L.); jevgeni.sablonin@ut.ee (E.S.); vaseugen42@mail.ru (E.V.)

<sup>3</sup> Karlsruhe Institute of Technology, Hermann-von-Helmholtz-Platz 1, Eggenstein-Leopoldshafen, D-76344 Karlsruhe, Germany; theo.scherer@kit.edu

\* Correspondence: kotomin@latnet.lv

**Abstract:** The radiation-induced optical absorption at 1.5–5.5 eV (up to the beginning of fundamental absorption) has been analyzed in CVD diamond disks exposed to 231-MeV <sup>132</sup>Xe ions with four fluences from 10<sup>12</sup> to 3.8 × 10<sup>13</sup> cm<sup>-2</sup>. The 5 mm diameter samples (thickness 0.4 mm) were prepared by Diamond Materials, Freiburg (Germany); the average grain size at growth site was around 80 μm; and the range of xenon ions was R = 11.5 μm. The intensity of several bands grows with ion fluence, thus confirming the radiation-induced origin of the defects responsible for these bands. The recovery of radiation damage has been investigated via isochronal (stepwise) thermal annealing procedure up to 650 °C, while all spectra were measured at room temperature. Based on these spectra, the annealing kinetics of several defects, in particular carbon vacancies (GR1 centers with a broad band ~2 eV) and complementary C-interstitial-related defects (~4 eV), as well as impurity-related complex defects (narrow bands around 2.5 eV) have been constructed. The experimental kinetics have also been analyzed in terms of the diffusion-controlled bimolecular reactions. The migration energies of tentatively interstitial atoms (mobile components in recombination process) are obtained, and their dependence on the irradiation fluences is discussed.

**Keywords:** CVD diamond; swift heavy ions; irradiation; Xe; optical absorption; Frenkel defects; interstitial ions; thermal annealing; diffusion-controlled reactions



**Citation:** Kotomin, E.A.; Kuzovkov, V.N.; Lushchik, A.; Popov, A.I.; Shablonin, E.; Scherer, T.; Vasil'chenko, E. The Annealing Kinetics of Defects in CVD Diamond Irradiated by Xe Ions. *Crystals* **2024**, *14*, 546. <https://doi.org/10.3390/cryst14060546>

Academic Editor: Weichao Bao

Received: 26 April 2024

Revised: 31 May 2024

Accepted: 8 June 2024

Published: 12 June 2024



**Copyright:** © 2024 by the authors. Licensee MDPI, Basel, Switzerland. This article is an open access article distributed under the terms and conditions of the Creative Commons Attribution (CC BY) license (<https://creativecommons.org/licenses/by/4.0/>).

## 1. Introduction

Optical and dielectric materials, both perfect and doped, play a key role in numerous high tech applications [1–3] and attract increasing attention for their modelling from the first principles [4,5]. In particular, diamond is a very attractive material, not only as a gemstone but also for fundamental science and innovative applications, such as quantum technologies, sensors, radiation detectors, nanoscale chemical and biomedical imaging, as well as applications in green and sustainable technologies [6–12]. Moreover, it is the material addressed in the major future research directions of the EU programme's Quantum Technologies Flagship [13] and Quantum Communication Infrastructure [14].

Diamond also has potential for use as a window in an electronic cyclotron heating system for a DEMO EUROfusion reactor, although production of a large-size diamond disk costs a six-digit amount. Unfortunately, it is possible that these expensive reactor windows fail. As the result, optical material failure can create a reactor safety problem, as windows are a fragile barrier between the very hot plasma and the reactor environment. Thus, it is important to ensure the high quality and controllability of the properties of these materials (including the effects of dopants and radiation-induced defects).

Diamond optical applications rely on unique properties and the existence of color centers, such as the vacancies V, combined with impurities: NV, SiV and other group IV vacancy centers. These centers can be used not only for sensing magnetic and electric fields but also for quantum information technology. However, progress in this field relies on substantial advances in the production of highly controlled diamond materials with low defect density, using chemical vapor deposition (CVD) or high-pressure, high-temperature (HPHT) techniques.

Besides that, an ultimate control of the material electronic properties is required in other application fields, for the development of diamond-based high-power devices. To achieve these goals and requirements, researchers are developing and optimizing reactors for diamond epitaxy, aiming at highly scalable and reproducible processes for quantum devices based on diamond, as well as analyzing the gas dynamics inside the reactors in-depth, for better control and optimization of the growth parameters. All of this is followed by an in-depth materials analysis, where the improvement of characterization techniques is essential for further advancement in the fascinating research field of diamond.

In many wide-gap materials (the majority of metal oxides, semiconductors), the formation energy of a vacancy–interstitial Frenkel pair exceeds the energy gap  $E_g$  by several times (see, e.g., [15], and references therein). Therefore, the Frenkel defects in these materials are predominantly created via the elastic collisions of energetic particles (electrons, neutrons, ions) with material nuclei, while the efficiency of ionization mechanisms is extremely low (in contrast, the decay of excitons and relaxed electron–hole pairs mainly lead to Frenkel defect creation in alkali halides) [16,17]. There is a large number of relevant publications on the creation/accumulation/annealing kinetics of radiation point defects in different wide-gap materials exposed to energetic ions (see, e.g., [18–20], and references therein). Using the optical absorption (or EPR) method, we determined the integrated amount of radiation defects (and then calculate their concentration) in a whole irradiated volume of the sample (in a thin layer in case of ion-irradiation). Note that the very high density of electronic excitations along swift heavy ion tracks definitely influences material mechanical properties and is responsible for the creation of expanded defects and lattice local disorder (see [21–23] and references therein).

In this paper, we study experimentally and theoretically the radiation properties of CVD diamond exposed to swift heavy ions with varying fluence, which is relevant for windows in fusion reactors. So far, mainly defects induced by electron- and light ion irradiation in CVD diamond were considered in the literature (see [21–23] and references therein).

## 2. Materials and Experimental Methods

The 5 mm diameter samples (thickness 0.4 mm) investigated in the present study have been fabricated via CVD plasma process at the company “Diamond Materials” (Freiburg, Germany). Due to the fabrication process, the grain size of polycrystalline diamond is rather different at two disk surfaces, as there is a conical structure due to the columnar growth, with increasing grain diameter from the nucleation site (at substrate) to the growth site. According to the electron backscatter diffraction method (EBSD) the average grain size by area checked at the growth site for our sample set is about 80–85  $\mu\text{m}$ .

The CVD diamond disks were exposed to 231-MeV  $^{132}\text{Xe}$  ions with four fluences  $\Phi$  from  $10^{12}$  to  $3.8 \times 10^{13} \text{ cm}^{-2}$ . The irradiation was performed at room temperature (RT) at the DC-60 accelerator in Astana, Kazakhstan. According to SRIM-2013 calculations [24], the range  $R$  of the Xe ions used is about 11.5  $\mu\text{m}$ , and this value determines the width of the sample layer with radiation-induced damage inside. The following EBSD measurements for the same samples after ion irradiation demonstrated that there is no influence on the microstructure caused by irradiation with Xe ions, independent of the fluence. Thus, the size of radiation-induced defects is on a much smaller scale than is detectable via the EBSD technique.

The spectra of optical absorption were measured at RT in a spectral range from 1.5 eV up to about 6.5 eV by means of a high-absorbance spectrometer JASCO V-660 for the same diamond disks before and after exposure to energetic ions. According to Figure 1, the absorption spectra of our pristine CVD diamond samples can be measured until the beginning of the diamond's fundamental absorption above 5.5 eV (the characteristic free exciton emission at 5.25 eV is detectable in low-temperature cathodoluminescence spectra, see, e.g., [12,25–27]). The absorption at lower exciting photon energies belongs to the so-called as-fabricated imperfections, including light scattering on the rather expanded structural defects and grain boundaries.

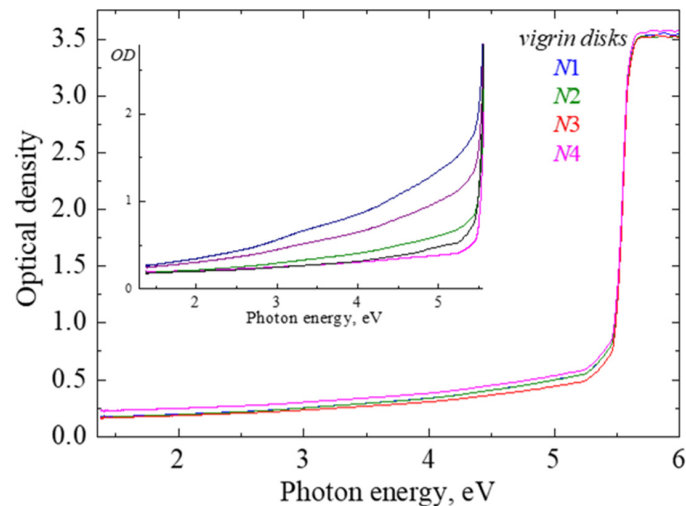


**Figure 1.** Absorption spectra measured for pristine CVD diamond disks N1–N4 at RT. Inset illustrates the examples of absorption (extinction) spectra for other pristine samples prepared under different fabrication conditions.

The inset in Figure 1 presents the absorption spectra of several earlier studied pristine CVD diamond samples, which illustrate that such “extrinsic” absorption/extinction often strongly depends on the technical features of the CVD procedure.

To avoid variations in the “background” absorption spectra of different samples before irradiation, the spectra of the so-called radiation-induced optical absorption (RIOA), where the spectrum of the pristine sample was subtracted from that measured for the same sample after irradiation, were used for the analysis of radiation damage in our CVD diamond disks. Note that the limiting value of optical density measurable via spectrophotometer is about  $OD = 3.5$ .

Figure 2 presents the spectra of RIOA measured at RT after the exposure of our four CVD diamond samples to 231-MeV xenon ions with varying fluence. The absorption spectra contain broad and complex radiation-induced bands spreading up to the beginning of fundamental absorption above 5.5 eV. Although the values of RIOA are extremely weak for the case of the lowest fluence, the intensity of broad and complex bands clearly increases (without any saturation sign) with irradiation fluence, thus confirming the radiation-induced origin of the relevant defects. Note that vacancy–interstitial Frenkel defect pairs are formed under irradiation, predominantly via the universal displacement mechanism (elastic collisions).

The carbon vacancies (noted as GR1 defects, neutral vacancies) are mainly responsible for the RIOA band around 2 eV; complementary C-interstitial-related defects R11 tentatively absorb at about 4 eV (see, e.g., [12,21,22]), while narrow bands around 2.5 eV are tentatively related to impurity-related complex defects. In particular, it could be some nitrogen-related defects [12,28,29], a number of which were detected in the Raman and FTIR spectra of the same pristine and Xe-irradiated CVD diamond samples (not considered in the present paper).

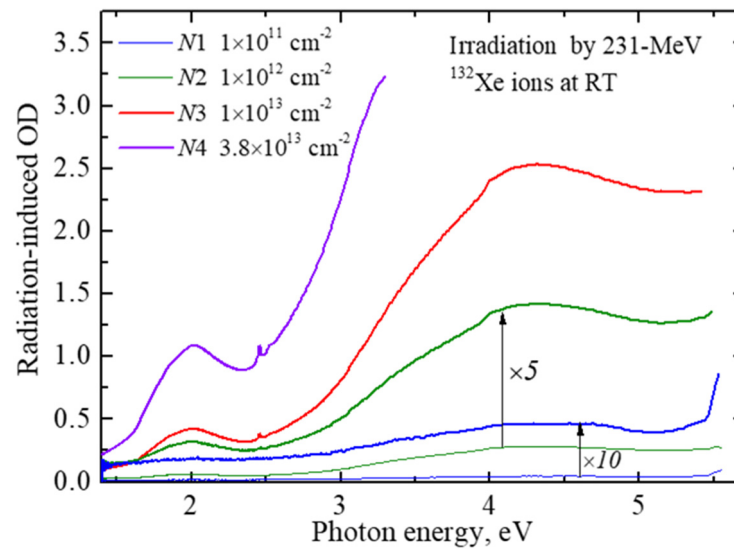


**Figure 2.** RIOA spectra of CVD diamond disks (absorption of pristine sample is subtracted) exposed to energetic Xe ions with different fluences at RT. For the best visualization, low-fluence curves are also multiplied by a certain factor.

The recovery of radiation damage, i.e., the determination of the thermal stability of radiation defects, has also been investigated via an isochronal (stepwise) thermal annealing procedure. An irradiated sample was heated in an argon atmosphere from RT to a certain temperature  $T_{pr}$ , kept at this temperature for 5 min, and then cooled down to RT by moving the quartz reactor tube with the sample out of the furnace. The absorption spectra were measured after each preheating at the same temperature, RT. Figure 3 demonstrates as examples a set of absorption spectra measured during such a preheating procedure, performed for the CVD disks irradiated with different fluences of xenon ions. For a better visualization of the changes in intensity of the narrow bands around 2.5 eV, the absorption spectrum at 1.4–2.6 eV is shown in Figure 4 (and the absorption of a pristine sample is not subtracted in this case).

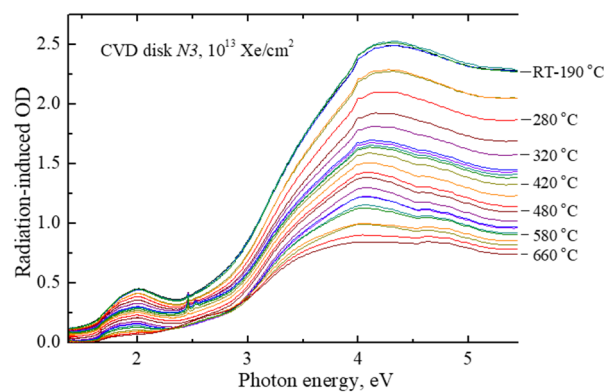


**Figure 3.** RIOA spectra of CVD diamond disk N3 exposed to 231-MeV xenon ions with fluence of  $10^{13} \text{ cm}^{-2}$  after irradiation (RT) and additional preheating to certain temperatures. All spectra are measured at RT.

Based on such sets of absorption spectra, the dependence of certain defect concentrations on the preheating temperature can be constructed if the relation of RIOA to the relevant defects in different spectral regions is established. Figure 5 demonstrates the temperature behavior of the concentration of radiation defects responsible for the two narrow RIOA bands around 2.5 eV (peak intensity at 2.46 or 2.52 eV above broad band absorbance is taken as a measure of relevant defects). The defect concentration first increases significantly at 250–320 °C, and the decay of both defect types occurs at 380–460 °C.

Such temperature dependence, with a rise stage, is typical of an additional formation of the defects (concentration increase), from the components of similar but less temperature-stable defects becoming mobile with a rise in temperature. A further analysis of the annealing behavior of relevant defects, the concentration of which is rather low especially in sample  $N_3$  (compare ordinate scales in two parts of Figure 5), still lies ahead and will be considered in a separate paper.

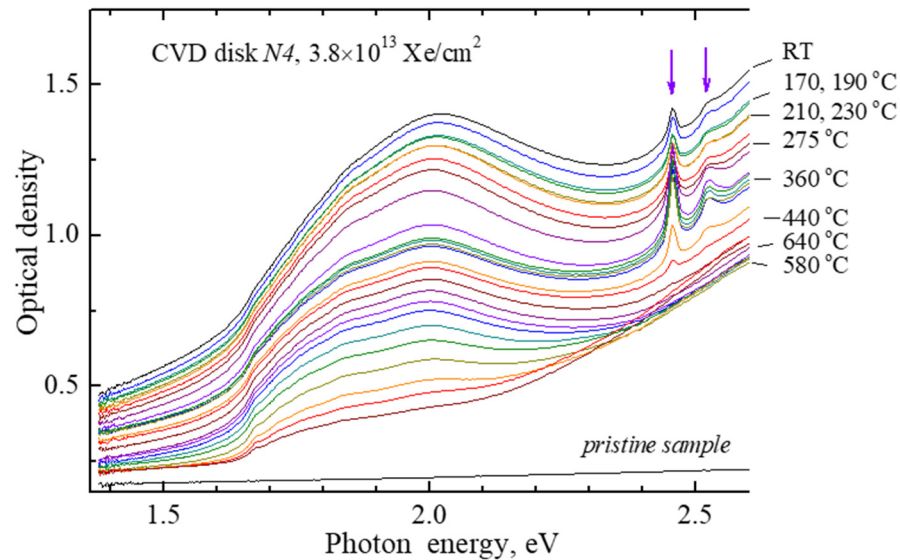


**Figure 4.** Absorption spectra of a CVD diamond disk  $N_4$  (as-measured, absorption of a pristine sample is not subtracted) exposed to Xe ions with fluence of  $3.8 \times 10^{13} \text{ cm}^{-2}$  after irradiation (RT) and additional preheating to certain temperatures. All spectra are measured at RT.

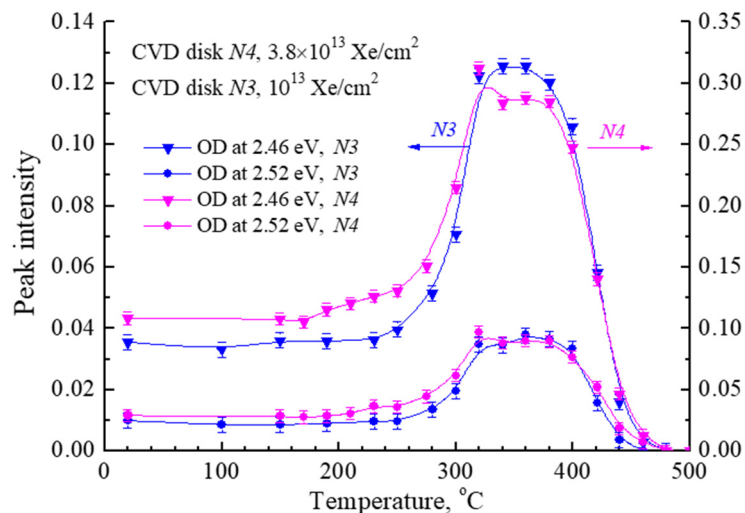


**Figure 5.** Annealing curves of two narrow bands around 2.5 eV (the peak OD values are taken at two different photon energies shown by arrows in Figure 4) in CVD diamond disks exposed to 231-MeV xenon ions with different fluences.

Figure 6 shows the difference spectra that represent the decrease in RIOA occurring between the two preheatings of the irradiated CVD diamond ( $10^{13} \text{ Xe/cm}^2$ ). Difference spectra show the correlation of the annealing of carbon vacancy-related defects (GR1) responsible for the broad RIOA band around 2 eV, with the decay of RIOA at around 4 eV connected with carbon–interstitial-related defects. So, these defects can be considered as complementary ones from the Frenkel pairs created at the elastic collision of incident



energetic ions with diamond crystal nuclei, and the interstitial mobility should cause their mutual recombination at the following heating of the irradiated sample.

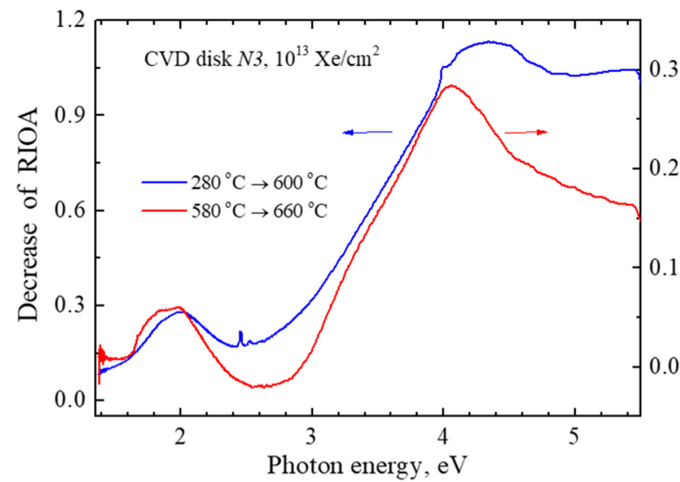


**Figure 6.** The difference spectra representing the decrease in RIOA occurred between two preheatings of the irradiated crystal ( $10^{13}$  Xe/cm<sup>2</sup>) from  $T_1$  to  $T_2$ .

Note that the precise separation of interstitial-related RIOA is rather complicated, because only two thirds of definitely complex RIOA around 4 eV are annealed at  $T_{pr} = 660$  °C, which is the limit of our measurements. According to our earlier experience with the annealing of radiation-induced damage in CVD diamond disks, the degradation of the CVD disks starts at  $T_{pr} > 700$  °C and leads to total loss of optical transparency and a rather intense swelling at higher  $T_{pr}$ . The first manifestations of CVD diamond degradation were also observed in our present samples at  $T_{pr} > 660$  °C (the noticeable rise of a background first starts at 2.3–3 eV and then covers a whole spectral region).

Nevertheless, we succeeded in measuring an almost total annealing process of the vacancy-related RIOA band around 2 eV in three samples irradiated by Xe ions, with fluences starting from  $\Phi = 10^{12}$  Xe/cm<sup>2</sup>. Figure 7 demonstrates the normalized dependences of the concentration of radiation-induced carbon vacancies (RIOA at 2 eV) on the preheating temperature in these irradiated CVD disks. The lowest fluence of  $\Phi = 10^{11}$  Xe/cm<sup>2</sup> does not cause RIOA sufficient for the analysis. Only these experimentally obtained kinetics curves will be analyzed in the next section, in terms of diffusion-stimulated bimolecular recombination reactions.

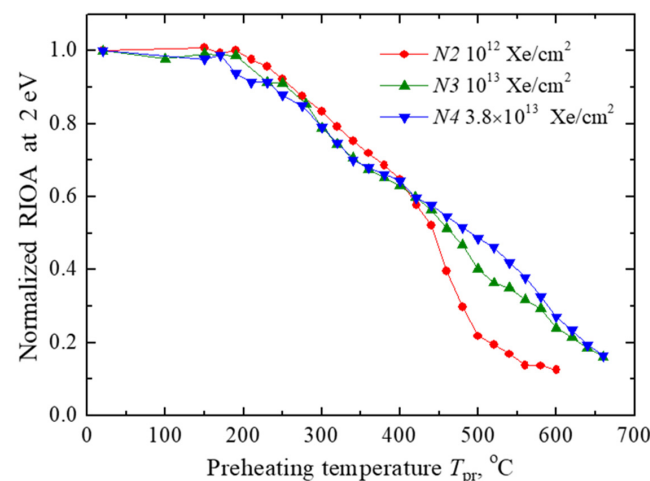


**Figure 7.** Normalized annealing curves of RIOA at 2 eV in CVD diamond disks exposed to 231-MeV xenon ions with varying fluence.

### 3. Theoretical

#### 3.1. Analysis of Kinetics

The annealing kinetics of radiation defects arises due to the recombination of Frenkel defects (vacancy–interstitial pairs, denoted here as  $F$  (vacancy) and  $H$  interstitial centers). Figure 7 shows the decay of concentrations, with  $C_i$  normalized to unity at low temperatures.

We consider the kinetics of bimolecular reaction: the change in the concentration of defects  $F, H$  is described by the following standard kinetic equation:

$$\frac{dn_F(t)}{dt} = \frac{dn_H(t)}{dt} = -K(t)n_F(t)n_H(t), \quad (1)$$

where  $K(t)$  is the recombination rate. For complementary Frenkel defects, we use the natural condition of equality of initial concentrations  $n_F(0) = n_H(0) = n_0$ , so for dimensionless defect concentrations  $C(t) = n_F(t)/n_0 = n_H(t)/n_0$

$$\frac{dC(t)}{dt} = -K(t)n_0C^2(t). \quad (2)$$

This equation can be easily integrated. Thus, the defect concentration decay is:

$$\frac{1}{C(t)} = 1 + n_0 \int_0^t K(t)dt. \quad (3)$$

Further, we use the well-known result of Smoluchowski [30–32] in the theory of diffusion-controlled processes: the diffusion-controlled reaction rate  $K$  is proportional to the mutual diffusion coefficient  $D = D_F + D_H$ ,

$$K = 4\pi DR, \quad (4)$$

where  $R$  is the recombination radius. As is well known, the mobility of interstitials is orders of magnitude greater than that of vacancies (the latter could be considered an immobile component in the recombination process considered [19,32,33]). Therefore, the kinetics is determined only by the mobility of interstitials,  $D = D_H$ , and the latter depends on temperature in the following standard way:

$$D = D_0 \exp\left(-\frac{E_a}{k_B T}\right), \quad (5)$$

through the activation energy of diffusion  $E_a$ .

Note that in Equation (3) the reaction rate  $K(t)$  has an argument  $t$ . The reason is obvious: during the cyclic heating (and cooling) of the sample, the reaction rate changes due to the trivial reason of temperature changes,  $T(t)$ , and the latter is included in Equation (4) through the diffusion coefficient, Equation (5), in combination with the activation energy of diffusion.

The integration in Equation (3) can be simplified. First of all, we note that during spectral studies, work is carried out at room temperature ( $T = T_R$ ). In this case, the mobility of the interstitials can also be neglected, considering them immobile. In other words, during spectral studies  $K(t) = 0$ , respectively, for kinetics these time intervals can simply be omitted. In the theoretical formula, only the process of stepwise heating can be left (redefinition of time).

The integral, over any small period of time  $\Delta t_0$  during which the sample remains in the thermostat at a fixed temperature  $T_j$ , is trivial and equal to  $K_j \Delta t_0$ , since in this interval the temperature is constant,  $T = T_j$ , as is the reaction rate  $K(t) = K_j$ . For the times the sample is in the thermostat at the temperature  $T_i$  of interest to us, the integral in Equation (3) is converted into the sum over the temperatures of all previous temperature steps, including the last one with temperature  $T_i$ . At this stage of the study, we are faced with the classical problem of mathematical analysis about the correspondence between the

sum (arising from the stepwise form of the temperature dependence) and the integral. The sum over temperature can be replaced by an integral, which is mathematically correct in the limit of a large number of experimental points. In other words, we assume that, in a correctly conducted experiment, the number of temperature points is large enough that the experimental results are meaningful and can be subjected to further analysis. We will see below that this assumption is confirmed by a comparison of theory and our experiment.

Formally, the result of the transition to the limit follows from Equation (3) with a standard replacement of the integration variable,  $dt = \left(\frac{dt}{dT}\right)dT$ . In the limiting transition to the integral, in a physical sense, the value  $\left(\frac{dt}{dT}\right)$  represents the average heating rate  $\beta$  of the sample in the thermostat during the transition from one temperature step to the next. It should be assessed as  $\beta = (T_{max} - T_R)/\Delta t$ , i.e., as the ratio of the temperature range under study to the total residence time of the sample in the thermostat.

Thus, we come to the final result (see also Ref. [33]) when the theory can already be compared with experiment:

$$\frac{1}{C_i} = 1 + 4\pi X \int_{T_R}^{T_i} e^{-\frac{E_a}{k_B T}} dT, \quad (6)$$

where

$$X = \frac{n_0 D_0 R}{\beta}. \quad (7)$$

Let us pay attention to a characteristic feature of the resulting expression. The temperature dependence of the concentration of defects is determined by the integral containing the activation energy of diffusion. This is a fundamental material parameter. All other physical parameters do not appear individually, but only as a product, see Equation (7). In other words, annealing kinetics fundamentally cannot provide information about the initial concentration of defects, or about the pre-exponential diffusion, since many of the parameters are, at best, estimated in the literature only in order of magnitude. At the same time, the value of the kinetic pre-factor  $X$ , as we will see, allows us to evaluate some trends associated with structural changes in irradiated materials. Equation (6) provides an answer to the previously posed question about the dependence of the results on the experimental conditions. As we see, this dependence manifests itself through the presence of the  $\beta$  parameter (the only significant parameter characterizing the experiment), but this parameter only determines the pre-exponential of the temperature dependence. These kinds of dependencies are usually classified as weak.

The resulting formula, Equation (6), allows us to process the experimental curves using the least squares method. As a result, each experimental kinetics will be characterized by two parameters,  $E_a$  and  $X$ . Before we analyze the experiment, we will estimate the expected value of the parameter  $X = X'$  (note that any large deviation from this expected result has important physical reasons, which we will discuss later). We proceed from the assumed (mainly in order of magnitude) parameter values:  $D_0 = 10^{-3} \text{ cm}^2 \text{ s}^{-1}$  (a typical estimate used for standard diffusion in solids);  $R = 10^{-7} \text{ cm}$  [31,32] (the typical radius of the spontaneous recombination of an interstitial with the vacancy it left); and the defect concentration  $n_0 = 10^{18} \text{ cm}^{-3}$ . The heating rate  $\beta \sim 0.1 \text{ K s}^{-1}$  (rounded, in our experiment). This results in an estimate  $X' \sim 10^8 \text{ K}^{-1}$ . Note that the experimental study [34] of self-diffusion in diamond suggested that  $D_0$  could be a few orders of magnitude larger, so our estimate could be the lower bound one.

### 3.2. Results

Figure 8 shows good agreement between the theory and the experiment. The results are quite convincing. It is obvious that the proposed theoretical scheme, Equation (6), works quite well. It is also obvious that the mathematical simplifications made in deriving Equation (6) are completely justified. At the same time, it should be taken into account that in addition to the usual errors in the experimental measurement of spectra, the uncontrolled



effect of sample degradation even at relatively low temperatures was superimposed on the experimental results. By the time the samples degrade, 20–40% of the defects have time to recombine (the annealing stage is far from completed). As is known, the accuracy of determining the activation energy depends on the temperature range used for the analysis. In our case, this interval is not large, so the accuracy of determining material characteristics by theoretical methods should not be overestimated.

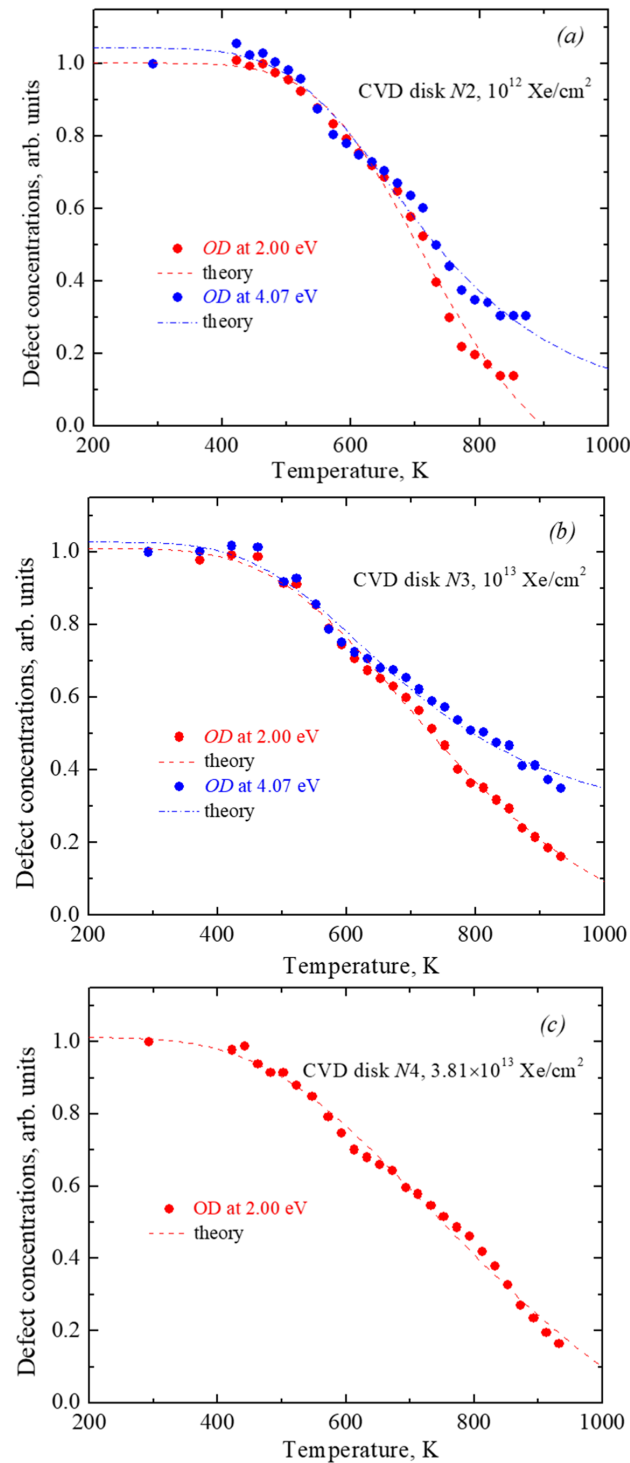


**Figure 8.** Annealing curves of RIOA at 2 eV and 4.07 eV in CVD diamond disks exposed to different Xe ion fluencies ((a)— $10^{12}$  cm<sup>-2</sup>; (b)— $10^{13}$  cm<sup>-2</sup>; (c)— $3.81 \times 10^{13}$  cm<sup>-2</sup>). Symbols—experiment point, lines—modelling in terms of diffusion-stimulated bimolecular recombination.

Using the least squares method, we find for each annealing curve a pair of parameters  $-E_a$  and  $X$ . We estimate the accuracy in the extraction of  $E_a$  and  $\ln(X)$  as 10%. The main uncertainty comes not from the fitting theory to experimental curves but from the experimental noise and gradual degradation of the material with heating. The results are systematized in Table 1.

**Table 1.** The obtained migrations energy of interstitials  $E_a$  and corresponding pre-exponential factors  $X$ .

Diamond Nr.	Band (eV)	Fluence, Xe/cm <sup>2</sup>	$E_a$ (eV)	Pre-Factor $X$ (K <sup>-1</sup> )
2	2.0	$10^{12}$	0.33	$1.2 \times 10^{-1}$
3	2.0	$10^{13}$	0.20	$8.7 \times 10^{-3}$
4	2.0	$3.8 \times 10^{13}$	0.15	$2.1 \times 10^{-3}$
2	4.07	$10^{12}$	0.27	$5.1 \times 10^{-2}$
3	4.07	$10^{13}$	0.20	$1.6 \times 10^{-3}$

It can be noted that in all variants the value of the parameter  $X$  differs significantly (by many orders of magnitude) from the estimate  $X' \sim 10^8 \text{ K}^{-1}$  (or even larger, as discussed above). This means that we are faced with a case of anomalous diffusion. Before we analyze this type of diffusion, let us note some patterns. Firstly, at a fixed fluence value, the activation energies for the two bands, 2.0 eV and 4.07 eV, coincide. They coincide exactly (within the accuracy of the method) at a fluence of  $10^{13} \text{ Xe/cm}^2$ , and differ slightly at a fluence of  $10^{12} \text{ Xe/cm}^2$  (the discrepancy between the values of 0.27 and 0.33 is not so great if we take into account the research under conditions of sample degradation). Secondly, at a fixed fluence value, the values of the  $X$  parameter also differ a little. Here it is necessary to clarify that in the case of parameters that can change by many orders of magnitude, it is not the parameters themselves that need to be compared, but their logarithms,  $\ln(X)$ . We will see below, in Figure 9, that studying the behavior of the  $\ln(X)$  value is of particular interest.

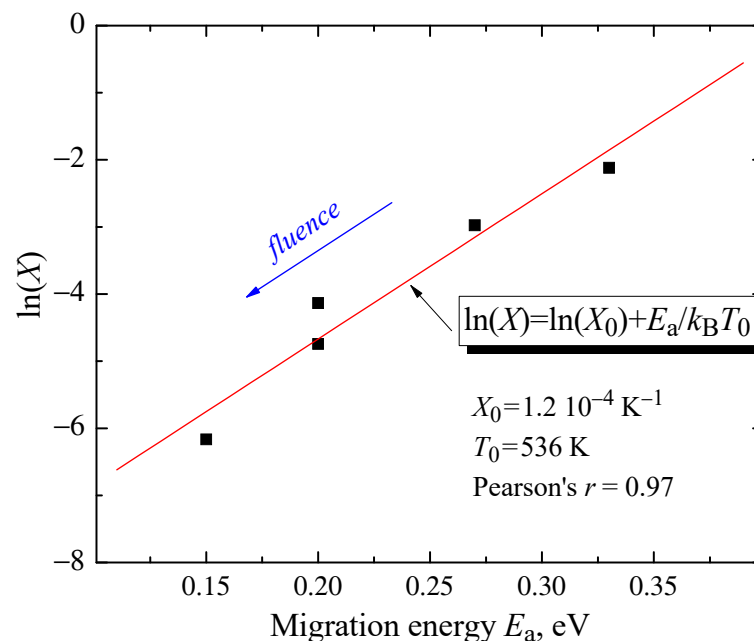


**Figure 9.** Correlation between the carbon interstitial migration energies  $E_a$  and pre-exponents  $X$ .

Thus, we have some confirmation of the considerations expressed just above (text related to Figure 6) about the correlation of the annealing kinetics of two absorption bands, 2.0 eV and 4.07 eV. Both bands result from the recombination of the same type of interstitial sites. An additional analysis (below) strengthens this claim. There is every reason to believe that bands at 2.0 eV and 4.07 eV form a kinetic doublet, so the results in Table 1 can be

combined and examined using statistical methods. The table reveals two effects. On the one hand, the activation energy of diffusion systematically decreases with increasing fluence. On the other hand, the values of the kinetic factor  $X$  also simultaneously change.

Let us plot the values of  $E_a$  and  $X$  collected in the table in coordinates  $(E_a, \ln(X))$ . Analysis shows that the corresponding points on the plane deviate very little from a simple linear relationship (see Figure 9):

$$\ln(X) = \ln(X_0) + E_a/k_B, \quad (8)$$

where  $X_0$  is a constant and  $T_0$  a characteristic temperature (these values are shown in the legend in figure). There is a linear *positive* correlation. The coefficient of this correlation (Pearson's  $r$ ) has the value of  $r = 0.97$ , which differs very little from  $r = 1$  (perfect correlation). We face here the case of a very strong correlation: all data points practically lie on a line, where  $\ln(X)$  decreases and  $E_a$  decreases.

The relationship between the activation energy  $E_a$  of a certain kinetic process and the pre-exponential  $X$ , Equation (9), is well known in the chemical literature as the Meyer–Neldel rule [35,36]. In the case of radiation defects, the fulfillment of this relation was confirmed by us for a group of ionic crystals ( $\text{Al}_2\text{O}_3$ ,  $\text{MgO}$ ,  $\text{MgF}_2$ ,  $\text{MgAl}_2\text{O}_4$ ) [33,37]. Note, however, that in the paper [33] we can talk about proof, since statistics based on a large number of independent experiments were used for each material. In our case of diamond, it would be incorrect to talk about a strong proof based on Figure 9. We are talking about predicting the behavior of materials based on a small number of experiments, which will allow for more targeted research in the future.

Since recombination radius, defect concentration and heating rate in factor  $X$ , Equation (7), cannot vary over many orders of magnitude, the dependence  $\ln(X)$  vs  $E_a$ , Equation (8), can also be interpreted as a revision of the traditional estimate for the diffusion coefficient given by Equation (5).

In the case of the Meyer–Neldel effect, we are faced with anomalous diffusion in disordered media when an increase in fluence leads to a systematic decrease in the activation energy of diffusion, but at the same time this decrease is accompanied by a correction in the value of the diffusion pre-exponential, which becomes dependent on the activation energy:

$$D \sim \exp(E_a/k_B T_0 - E_a/k_B T). \quad (9)$$

This correlation is widely acknowledged across disciplines such as chemistry, biology, and semiconductor physics [36,38]. However, the underlying principles of this empirical rule remain incompletely understood. One conceivable phenomenological model proposed by Dyre [39] suggests that Equation (8) applies to disordered systems characterized by an exponential probability distribution of the energy barriers of localized quasi-particles, with the parameter  $T_0$  potentially indicating a glass transition. Equation (8) is typically observed in multicomponent systems. Our findings suggest that this phenomenon may also be applicable to simpler systems without altering their composition. Similar observations have been documented in glasses subjected to weak neutron or ion irradiation, where the activation energies exhibit only minor variations [40] (chalcogenide glass), [38] (metallic glass).

We note one more detail. In Ref. [33], characteristic temperatures  $T_0$  were determined for three ionic materials. It is fundamentally important that in all cases the study of annealing kinetics was carried out under the condition  $T < T_0$ . That is, the point defects were almost completely annealed before reaching the characteristic temperature. In the case of diamond, on the contrary, the experiment was partially carried out at temperatures higher than the characteristic temperature  $T_0$ . However, complete annealing could not be carried out due to degradation of the material. It is possible that the characteristic temperature (also known as the glass transition temperature in Ref. [39]) can also be compared to the degradation temperature.

#### 4. Conclusions

The variation in the spectra of diamond optical absorption in a wide range of 1.5–5.5 eV due to the energetic Xe ion irradiation, as well as during a further thermal annealing procedure up to 650 °C of the irradiated CVD diamond samples (from Diamond Materials, Freiburg, Germany), has been studied experimentally. The radiation-induced origin of the defects responsible for several bands has been confirmed and the annealing curves for the radiation-induced defects responsible for the optical absorption around 2 eV, 2.5 eV and 4.1 eV (including vacancies and interstitials) have been experimentally constructed.

A theoretical analysis of the experimental kinetics of the basic radiation defects (interstitial–vacancy carbon Frenkel defects responsible for the absorption at 4.1 eV and 2.0 eV, respectively) in CVD diamond disks shows the migration energy of the interstitial ions as quite low, of the order of 0.2–0.4 eV. The obtained migration energies are considerably smaller than those observed in the self diffusion of non-irradiated diamond [41], which could be related to a strong structural distortion upon heavy swift ion irradiation. This is confirmed by a variation in the migration energies with the fluence (Figure 9) and the very small values of extracted pre-factor parameters  $X$  in Table 1. This result needs further quantum mechanical calculations [42]. The decrease in the interstitial migration energy with the radiation fluence was observed earlier for  $\text{Al}_2\text{O}_3$ ,  $\text{MgO}$ , and  $\text{MgF}_2$  [33], and is a manifestation of the anomalous diffusion [33]. We assume that the local structure of irradiated solids is strongly disordered and to some degree is similar to liquids [43], where both the activation energies of diffusion and its pre-exponentials are much smaller than in solids. Similar phenomena were observed in disordered semiconductors and glasses (see more in [33]).

**Author Contributions:** Conceptualization A.I.P. and E.A.K.; methodology V.N.K. and A.L.; formal analysis V.N.K., T.S. and E.S.; writing—A.L. and V.N.K.; visualization E.S. and E.V.; supervision E.A.K. and V.N.K. All authors have read and agreed to the published version of the manuscript.

**Funding:** This study was supported by EUROfusion Enabling Research Project ENR-MAT.01.UT-T001-D001 “Investigation of defects and disorder in nonirradiated and irradiated Doped Diamond and Related Materials for fusion diagnostic applications (DDRM)—Theoretical and Experimental analysis.” This work has been carried out within the framework of the EUROfusion Consortium, funded by the European Union via the Euratom Research and Training Programme (Grant Agreement No 101052200—EUROfusion). Views and opinions expressed are, however, those of the author(s) only and do not necessarily reflect those of the European Union or the European Commission. Neither the European Union nor the European Commission can be held responsible for them. The research was partly performed in the Center of Excellence of the Institute of Solid State Physics, University of Latvia, supported through European Union’s Horizon 2020 Framework Programme H2020-WIDESPREAD-01-2016-2017-TeamingPhase2 under grant agreement No. 739508, project CAMART2.

**Data Availability Statement:** The data presented in this study are available on request from the corresponding author due to privacy.

**Acknowledgments:** Authors thank R. Vila and A. Platonenko for fruitful discussions.

**Conflicts of Interest:** The authors declare no conflicts of interest.

#### References

1. Pintsuk, G.; Aiello, G.; Dudarev, S.L.; Gorley, M.; Henry, J.; Richou, M.; Vila, R. Materials for in-vessel components. *Fusion Energy Des.* **2022**, *174*, 112994. [CrossRef]
2. Delgado, D.; Vila, R. Hydrogen species in diamond: Molecular dynamics simulation in bulk diamond for fusion applications. *J. Nucl. Mat.* **2014**, *452*, 218–222. [CrossRef]
3. Lushchik, A.; Dolgov, S.; Feldbach, E.; Pareja, R.; Popov, A.; Shablonin, E.; Seeman, V. Creation and thermal annealing of structural defects in neutron-irradiated  $\text{MgAl}_2\text{O}_4$  single crystals. *Nucl. Instr. Meth. B* **2018**, *435*, 31–37. [CrossRef]
4. Aiello, G.; Scherer, T.; Avramidis, K.; Casal, N.; Franke, T.; Gagliardi, M.; Woerner, E. Diamond window technology for electron cyclotron heating and current drive: State of the art. *Fusion Sci. Technol.* **2019**, *75*, 719–729. [CrossRef]

5. Dovesi, R.; Erba, A.; Orlando, R.; Zicovich-Wilson, C.M.; Civalieri, B.; Maschio, L.; Rérat, M.; Casassa, S.; Baima, J.; Salustro, S.; et al. Quantum-mechanical condensed matter simulations with CRYSTAL. *Wiley Interdiscip. Rev. Comput. Mol. Sci.* **2018**, *8*, e1360. [[CrossRef](#)]
6. Santos, N.; Figueira, F.; Neto, M.; Paz, F.A.A.; Braga, S.; Mendes, J. Diamonds for Life: Developments in Sensors for Biomolecules. *Appl. Sci.* **2022**, *12*, 3000. [[CrossRef](#)]
7. Field, J.E. *The Properties of Natural and Synthetic Diamond*; Academic Press: London, UK, 1992.
8. Szunerits, S.; Nebel, C.E.; Hamers, R.J. Surface functionalization and biological applications of CVD diamond. *MRS Bull.* **2014**, *39*, 517–524. [[CrossRef](#)]
9. Raymakers, J.; Haenen, K.; Maes, W. Diamond surface functionalization: From gemstone to photoelectrochemical applications. *J. Mater. Chem. C* **2019**, *7*, 10134–10165. [[CrossRef](#)]
10. Nasladek, M.; Pobedinskas, P. Recent Advances in Diamond Science and Technology: From Quantum Fundamentals to Applications. *Phys. Stat. Sol. A* **2023**, *220*, 2300051.
11. Pan, L.S.; Kania, D.R. *Diamond: Electronic Properties and Applications*; Springer Science & Business Media: Berlin, Germany, 2013.
12. Zaitsev, A.M. *Optical Properties of Diamond. A Data Handbook*; Springer: Berlin/Heidelberg, Germany, 2001.
13. Available online: <https://qt.eu> (accessed on 7 June 2024).
14. Available online: <https://digital-strategy.ec.europa.eu/en> (accessed on 7 June 2024).
15. Zinkle, S.J.; Kinoshita, C. Defect production in ceramics. *J. Nucl. Mater.* **1997**, *251*, 200–217. [[CrossRef](#)]
16. Nordlund, K.; Zinkle, S.J.; Sand, A.E.; Granberg, F.; Averbach, R.S.; Stoller, R.E.; Suzudo, T.; Malerba, L.; Banhart, F.; Weber, W.J.; et al. Primary radiation damage: A review of current understanding and models. *J. Nucl. Mater.* **2018**, *512*, 450–479. [[CrossRef](#)]
17. Itoh, N.; Duffy, D.M.; Khakshouri, S.; Stoneham, A.M. Making tracks: Electronic excitation roles in forming swift heavy ion tracks. *J. Phys. Condens. Matter* **2009**, *21*, 474205. [[CrossRef](#)]
18. Kuzovkov, V.N.; Kotomin, E.A.; Lushchik, A.; Popov, A.I.; Shablonin, E. The annealing kinetics of the F-type defects in MgAl<sub>2</sub>O<sub>4</sub> spinel single crystals irradiated by swift heavy ions. *Opt. Mater.* **2024**, *147*, 114733. [[CrossRef](#)]
19. Lushchik, A.; Feldbach, E.; Kotomin, E.A.; Kudryavtseva, I.; Kuzovkov, V.N.; Popov, A.I.; Seeman, V.; Shablonin, E. Distinctive features of diffusion-controlled radiation defect recombination in stoichiometric magnesium aluminate spinel crystals and transparent polycrystalline ceramics. *Sci. Rep.* **2020**, *10*, 7810. [[CrossRef](#)]
20. Baubekova, G.; Akilbekov, A.; Kotomin, E.A.; Kuzovkov, V.N.; Popov, A.I.; Shablonin, E.; Lushchik, A. Thermal annealing of radiation damage caused by swift <sup>132</sup>Xe ions in MgO single crystals. *Nucl. Instrum. Meth. B* **2020**, *462*, 163–168.
21. Iakoubovskii, K.; Kiflawi, I.; Johnston, K.; Collins, A.; Davies, G.; Stesmans, A. Annealing of vacancies and interstitials in diamond. *Phys. B* **2003**, *340*, 67–75. [[CrossRef](#)]
22. Green, B.L.; Collins, A.T.; Breeding, C.M. Diamond spectroscopy, defect centers, color, and treatment. *Rev. Mineral. Geochem.* **2022**, *88*, 637–688. [[CrossRef](#)]
23. Collins, A.T. Optical centers produced in diamond by radiation damage. *N. Diam. Front. C Tec.* **2007**, *17*, 47–61.
24. Ziegler, J.F.; Ziegler, M.D.; Biersack, J.P. SRIM—The stopping and range of ions in matter. *Nucl. Instrum. Meth. B* **2010**, *268*, 1818–1823. [[CrossRef](#)]
25. Dean, P.J. Bound excitons and donor-acceptor pairs in natural and synthetic diamond. *Phys. Rev.* **1965**, *139*, A588–A602. [[CrossRef](#)]
26. Collins, A.T.; Kamo, M.; Sato, Y. Intrinsic and extrinsic cathodoluminescence from single-crystal diamonds grown by chemical vapour deposition. *J. Phys. Cond. Matter.* **1989**, *1*, 4029–4033. [[CrossRef](#)]
27. Takeuchi, D.; Watanabe, H.; Yamanaka, S.; Okushi, H.; Sawada, H.; Ichinose, H.; Sekiguchi, T.; Kajimura, K. Origin of band-A emission in diamond thin films. *Phys. Rev. B* **2001**, *63*, 245328. [[CrossRef](#)]
28. Collins, A.T.; Connor, A.; Ly, C.-H.; Shareef, A.; Spear, P.M. High-temperature annealing of optical centers in type-I diamond. *J. Appl. Phys.* **2005**, *97*, 083517. [[CrossRef](#)]
29. Nadala, L.; Grambole, D.; Wildner, M.; Gigler, A.M.; Hainschwang, T.; Zaitsev, A.M.; Harris, J.W.; Milledge, J.; Schulze, D.J.; Hofmeister, W.; et al. Radio-colouration of diamond: A spectroscopic study. *Contrib. Miner. Pet.* **2013**, *165*, 843–861. [[CrossRef](#)]
30. Smoluchowski, M.V. Versuch einer mathematischen Theorie der Koagulationskinetik kolloider Lösungen. *Z. Phys. Chem. B* **1917**, *92*, 129–168. [[CrossRef](#)]
31. Kotomin, E.A.; Kuzovkov, V.N. Phenomenological kinetics of Frenkel defect recombination and accumulation in ionic solids. *Rep. Prog. Phys.* **1992**, *55*, 2079. [[CrossRef](#)]
32. Kotomin, E.A.; Kuzovkov, V.N. *Modern Aspects of Diffusion-Controlled Reactions*; Series of Comprehensive Chemical Kinetics; Elsevier: Amsterdam, The Netherlands, 1996; Volume 34.
33. Kotomin, E.; Kuzovkov, V.; Popov, A.I.; Maier, J.; Vila, R. Anomalous kinetics of diffusion-controlled defect annealing in irradiated ionic solids. *J. Phys. Chem. A* **2018**, *122*, 28–32. [[CrossRef](#)] [[PubMed](#)]
34. Koga, K.T.; Walter, M.J.; Nakamura, E.; Kobayashi, K. Carbon self-diffusion in natural diamond. *Phys. Rev. B* **2005**, *72*, 024108. [[CrossRef](#)]
35. Meyer, W.; Neldel, H. Concerning the relationship between the energy constant epsilon and the quantum constant alpha in the conduction-temperature formula in oxydising semi conductors. *Phys. Z.* **1937**, *38*, 1014–1019.
36. Jones, A.G. Compensation of the Meyer-Neldel Compensation Law for H diffusion in minerals. *Geochem. Geophys. Geosyst.* **2014**, *15*, 2616–2631. [[CrossRef](#)]

37. Lushchik, A.; Kuzovkov, V.; Popov, A.I.; Prieditis, G.; Seeman, V.; Shablonin, E.; Vasil'chenko, E.; Kotomin, E.A. Evidence for the formation of two types of oxygen interstitials in neutron-irradiated  $\alpha$ -Al<sub>2</sub>O<sub>3</sub> single crystals. *Sci. Rep.* **2021**, *11*, 20909. [[CrossRef](#)] [[PubMed](#)]
38. Mehta, N.; Singh, K.; Saxena, N.S. Correlation between pre-exponential factor and activation energy of non-isothermal crystallization for virgin and irradiated Fe<sub>78</sub>B<sub>13</sub>Si<sub>9</sub> metallic glass. *Phys. B* **2009**, *404*, 2184. [[CrossRef](#)]
39. Dyre, J.C. A phenomenological model for the Meyer–Neldel rule. *J. Phys. C Solid State Phys.* **1986**, *19*, 5655–5664. [[CrossRef](#)]
40. Mehta, N.; Singh, K.; Saxena, N.S. Effect of slow neutron radiation on the pre-exponential factor of thermally activated crystallization in Se<sub>96</sub>In<sub>4</sub> chalcogenide glass. *J. Phys. D Appl. Phys.* **2008**, *41*, 135406. [[CrossRef](#)]
41. Jones, R.; Goss, J.P.; Pinto, H.; Palmer, D.W. Diffusion of nitrogen in diamond and formation of A-centers. *Diam. Relat. Mater.* **2015**, *53*, 35–39. [[CrossRef](#)]
42. Colasuonno, F.; Centile, F.; Mackrodt, W.; Ferrari, A.; Platonenko, A.; Dovesi, R. Interstitial defects in diamond. *J. Chem. Phys.* **2020**, *153*, 024119. [[CrossRef](#)]
43. Frenkel, J. *Kinetic Theory of Liquids*; London, Oxford University Press: Oxford, UK, 1946.

**Disclaimer/Publisher's Note:** The statements, opinions and data contained in all publications are solely those of the individual author(s) and contributor(s) and not of MDPI and/or the editor(s). MDPI and/or the editor(s) disclaim responsibility for any injury to people or property resulting from any ideas, methods, instructions or products referred to in the content.